Original Article

Value of an expanded range of lesions on contrast-enhanced ultrasound for the diagnosis of hypervascular breast masses

Chao Jia[#], Qinghua Niu[#], Long Liu, Gang Li, Lifang Jin, Lianfang Du, Qiusheng Shi, Fan Li

Department of Ultrasound, Shanghai General Hospital, Shanghai Jiao Tong University School of Medicine, Shanghai, China

Contributions: (I) Conception and design: F Li, Q Shi; (II) Administrative support: Q Shi, F Li, L Du; (III) Provision of study materials or patients: C Jia; (IV) Collection and assembly of data: C Jia, Q Niu, G Li; (V) Data analysis and interpretation: Q Niu, L Jin, L Liu; (VI) Manuscript writing: All authors; (VII) Final approval of manuscript: All authors.

[#]These authors contributed equally to this work.

Correspondence to: Fan Li, MD, PhD; Qiusheng Shi, MD, PhD. Department of Ultrasound, Shanghai General Hospital, Shanghai Jiao Tong University School of Medicine, 650 Xin Song Jiang Road, Shanghai 201620, China. Email: medicineli@163.com; sqs19631989@163.com.

Background: Breast cancer lesions show an expanded range on contrast-enhanced ultrasound (CEUS). Here, we quantitatively analyze this index to explore its effective cutoff value for distinguishing benign and malignant lesions and the corresponding diagnostic performance and investigate its role in prognostic assessment of malignant lesions.

Methods: Consecutive patients who underwent CEUS for breast lesions during the period from September 2017 to June 2019 were included. Original CEUS images were selected, displayed in dual-frame mode, and measured when enhancement of the lesion reached its peak. The longitudinal diameter, transverse diameter, and area of the lesion on the two-dimensional images and the corresponding postenhancement images were measured to calculate six indicators: longitudinal diameter increment, transverse diameter increment, area increment, percent increase in longitudinal diameter, percent increase in transverse diameter, and percent increase in area increment. With postoperative pathology as the gold standard, the cutoff values for distinguishing benign and malignant lesions and the correlations of these indicators with pathological subtypes and pathological grades were evaluated.

Results: Malignant lesions showed a more significantly expanded range after enhancement compared to benign lesions, especially in terms of area increase. When the cutoff value of the area increment was set at 0.47 cm^2 for distinguishing between benign and malignant lesions, the area under the curve (AUC) was 0.945, and the sensitivity, specificity, accuracy, positive predictive value, and negative predictive value were 90.1%, 91.5%, 90.9%, 87.2%, and 93.5%, respectively. The pathologically measured maximum diameter of malignant masses correlated with the percent increase in transverse diameter, area increment, and percent increase in area increment. The longitudinal diameter increment in the luminal A group was significantly smaller than that in the human epidermal growth factor receptor 2 (HER2)+ group. The percent increase in transverse diameter was helpful for predicting the pathological grade of malignant masses. When the cutoff value of the percent increase in transverse diameter was set at 10.84% for pathological grading, the AUC was 0.623, and the sensitivity was 90.8%.

Conclusions: Indicators related to the expanded lesion range on CEUS are helpful in differential diagnosis of benign and malignant lesions and in prognostic assessment of pathological grades.

Keywords: Contrast-enhanced ultrasound (CEUS); breast nodules; enhancement range; quantitative analysis

Submitted Apr 25, 2023. Accepted for publication Jun 05, 2023. Published online Jun 19, 2023.
doi: 10.21037/gs-23-165
View this article at: https://dx.doi.org/10.21037/gs-23-165

Introduction

Breast cancer is one of the most common malignant tumors worldwide. In 2020, there were approximately 2.3 million new breast cancer cases globally, representing 11.7% of all cancer cases; moreover, breast cancer was the fifth leading cause of cancer death, accounting for 685,000 deaths (1). The incidence of female breast cancer is rising in almost all countries, with an average annual growth rate of approximately 2% (2). Among all imaging techniques, ultrasound has the advantages of high resolution, simple operation, and no radiation injury and thus has been widely applied. Moreover, ultrasound is a particularly sensitive examination tool for Chinese women who have relatively small and dense breasts (3-5). Developed from two-dimensional ultrasound, contrast-enhanced ultrasound (CEUS) is a relatively new technique that has been developed in the last two decades, enabling display of the perfusion of contrast agent in the microvasculatures of lesions in a dynamic and real-time manner. Since breast cancer often manifests with abundant neovascularization (6), a previous study has demonstrated the potential of CEUS in differential diagnosis of benign and malignant breast tumors and in predicting the prognosis of malignant lesions (7). Furthermore, CEUS has many specific signs for malignant breast lesions, such as the degree of contrast enhancement, order-of-magnitude enhancement, internal homogeneity, border delineation, peripheral vascularity, and expanded lesion range, among which the expanded range after enhancement is the sign with higher specificity and is highly consistent with pathological findings (8,9). However, although its clinical diagnostic significance has been proposed, few in-depth studies have been performed. The thresholds of the expanded range for breast lesions remain controversial, and there is a lack of uniform diagnostic criteria for CEUS. The aim of this study was to determine a criterion for expanded range after enhancement and to investigate the relationship between expanded range after enhancement and the pathology-based gold standard. We present this article in accordance with the STARD reporting checklist (available at https://gs.amegroups.com/article/view/10.21037/gs-23-165/rc).

Highlight box

Key findings

- Indicators related to the expanded lesion range on contrast-enhanced ultrasound (CEUS) help diagnose breast lesions and assess pathological grades.

What is known and what is new?

- The expanded range after enhancement is key evidence for distinguishing a benign from a malignant breast tumor
- The present study found that the area increment was highly valuable. The longitudinal diameter increment in the luminal A group was significantly smaller than that in the human epidermal growth factor receptor 2 (HER2)+ group. The percent increase in transverse diameter was helpful for predicting the pathological grade of malignant masses.

What is the implication, and what should change now?

- When we make the diagnosis of breast lesions after CEUS, we can pay attention to the area increase value, longitudinal diameter increase value and transverse diameter increase percentage, which will be helpful for our prediction.

Methods

Subjects

In this single-center retrospective study, CEUS data for 512 breast nodules in 488 consecutive patients who underwent breast ultrasonography at hospital from September 2017 to June 2019 were analyzed. The inclusion criteria were as follows: (I) the breast lesion surgically removed and pathologically confirmed as benign or malignant; (II) complete clinical data, with pathological grading, molecular typing, and immunohistochemical results available for patients with malignant tumors; (III) ultrasound (US) and CEUS; (IV) high-quality images clearly displaying the lesions and the complete perfusion process on CEUS; (V) peak enhancement of lesions on CEUS higher than that of the surrounding breast tissue and exactly reflecting the lesion boundary; (VI) the interval between CEUS and surgical excision not exceeding 1 month; (VII) for patients with multiple nodules, other nodules re-examined by CEUS at 15-minute intervals after CEUS of one nodule; (VIII) no puncture or neoadjuvant therapy performed prior to CEUS; (IX) and informed consent. The exclusion criteria included the following: (I) incomplete clinical data; (II) lesion boundaries not be determined on CEUS, including peak enhancement similar to or below the surrounding tissues; (III) unclear image display, with no clear diagnosis; (IV) an interval between CEUS and surgical excision exceeding 1 month; (V) puncture or neoadjuvant therapy prior to CEUS. The study was conducted in accordance with the Declaration of Helsinki (as revised in 2013). The study was approved by institutional ethics board of Shanghai General

Hospital (No. 2016KY221) and individual consent for this retrospective analysis was waived.

Examination instruments and methods

An Aplio 500 (Canon, Japan) and Aplio i900 (Canon, Japan) equipped with 14-5 L and 14-8 L probes with working frequencies of 5–14 and 8–14 MHz, respectively, were used. The CEUS frequency was 5 MHz, and the mechanical index (MI) was 0.07. The patient was asked to assume the supine position, with both upper limbs elevated. The probe was placed gently over the breast skin. First, a conventional ultrasound scan was performed, during which the conventional sonographic presentation of the lesion was recorded. After the largest section of the lesion was selected and the probe was fixed, the contrast enhancement mode was entered. The dual-frame mode was selected to avoid deflection of the lesion, with the probe remaining fixed throughout the enhancement process. A bolus (4.8 mL) of contrast agent (SonoVue, Bracco, Milan, Italy) was injected via the median cubital vein, followed by the injection of 5 mL of normal saline. The observation lasted 1 min. The video recording was started simultaneously when the contrast agent was injected, and the images were saved in DICOM format.

Analysis of ultrasound images

Original CEUS images were selected, displayed in dual-frame mode, and measured when enhancement of the lesion reached its peak. The longitudinal diameter (d1), transverse diameter (d2), and area (s) of the lesion shown in the grayscale images were measured separately, and the area was calculated by the software installed in the machine. The longitudinal diameter (D1), transverse diameter (D2), and area (S) of the lesion after enhancement were also measured. Then, the following indicators were calculated: the longitudinal diameter increment ($\Delta d1 = D1 - d1$), transverse diameter increment ($\Delta d2 = D2 - d2$), area increment ($\Delta s = S - s$), percent increase in longitudinal/transverse diameter $[(D - d)/d \times 100\%]$, and percent increase in area increment $[(S - s)/s \times 100\%]$. The clinical data and pathological results of the lesions were concealed before measurement. The measurements were performed independently by two physicians with more than 5 years of experience in CEUS diagnosis, and the results were averaged. In cases of disagreement, a third physician with more than 8 years of experience in CEUS diagnosis was consulted to reach a final decision.

Pathological findings

The maximum diameter of the tumor was measured on the postoperative pathological gross specimen. Based on nuclear features (including the size and polarization of the nucleus, presence and size of nucleoli, and mitogram), breast cancer was pathologically divided into grade I–II and grade III groups (10). Molecular subtyping was based on the American Joint Committee on Cancer (AJCC) classification system (11). These lesions were classified as luminal A, luminal B, human epidermal growth factor receptor 2 (HER2)+, and triple-negative breast cancer (TNBC) according to estrogen receptor (ER), progesterone receptor (PR), and HER2 status.

Statistical analysis

SPSS 25.0 (IBM, USA) and GraphPad Prism 7.0 (GraphPad Software, USA) were used for statistical analysis. Measurement data (e.g., age) are presented as the mean ± standard deviation (SD), and count data are expressed in case numbers and percentages (n, %). Intergroup comparisons (benign *vs.* malignant lesions) were based on the rank sum test. Logistic regression was used to explore independent risk factors for diagnosis of malignant masses by CEUS. A receiver operating characteristic (ROC) curve was constructed for the area increment of malignant masses. The cutoff value between benign and malignant masses was assessed based on the Yordon index, and the sensitivity, specificity, accuracy, positive predictive value, and negative predictive value for diagnosis of benign/malignant masses were calculated. Correlations between the maximum diameter of malignant masses and each indicator related to expanded range were analyzed by Spearman analysis. The molecular subtypes included luminal A, luminal B, HER2 overexpression, and TNBC. Among these four groups, the area increment, transverse diameter increment, and percent increase in transverse diameter were normally distributed, and therefore, intergroup comparisons were based on analysis of variance. In contrast, distributions of percent increase in area increment, longitudinal diameter increment, and percent increase in longitudinal diameter were skewed, and their comparisons were based on the rank sum test. Furthermore, the indicators with intergroup differences were compared after Bonferroni correction. The lesions were divided into grade I–II and grade III

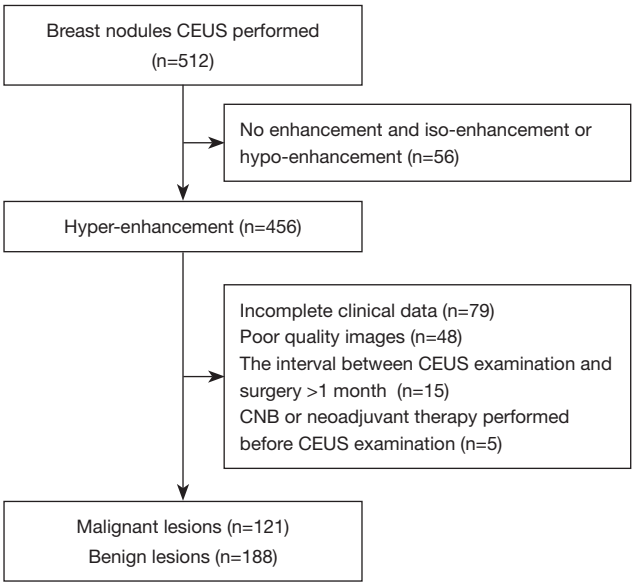

Figure 1 Flowchart of the study population and exclusion process. CEUS, contrast-enhanced ultrasound; CNB, core needle biopsy.

Table 1 Patient and tumor characteristics

Characteristics	Number (%) (n=309)
Patients	289
Tumors	309*
Age (years), mean ± SD (range)	46.5±13.6 (21 to 95)
Histological type, n (%)	
Benign lesion	188 (60.84)
Malignant lesion	121 (39.16)
IDC	118 (38.19)
Other	3 (0.97)
Pathological grade of malignant lesion, n (%)	
I	11 (3.60)
II	54 (17.48)
III	56 (18.12)
Molecular type of malignant lesion, n (%)	
Luminal A	25 (8.10)
Luminal B	62 (20.06)
HER2+	21 (6.80)
TNBC	13 (4.21)

*, 20 of 289 patients had two breast lesions. SD, standard deviation; IDC, invasive ductal carcinoma; HER2, human epidermal growth factor receptor 2; TNBC, triple-negative breast cancer.

groups according to the pathological grades. Between these two groups, the longitudinal diameter increment, transverse diameter increment, and area increment and their comparisons were based on *t*-tests. Distributions of percent increase in longitudinal diameter, percent increase in transverse diameter, and percent increase in area increment were skewed, and the rank sum test was applied. A ROC curve was constructed for the percent increase in transverse diameter. The cutoff value between benign and malignant masses was assessed based on the Yordon index, and the sensitivity, specificity, accuracy, positive predictive value, and negative predictive value for diagnosis of benign/malignant masses were calculated. A P value of <0.05 was considered statistically significant.

Results

According to the inclusion criteria, 309 nodules in 289 patients aged 21–95 (46.5±13.6) years were included in the analysis. The process of nodule screening is illustrated in *Figure 1*. Most of the malignant masses were infiltrating ductal carcinoma (IDC) (n=118, 38.19%). Among the malignant masses, grades I, II, and III accounted for 3.60% (n=11), 17.48% (n=54), and 18.12% (n=56), respectively. Molecular typing showed that the number and percentage of luminal A, luminal B, HER2 overexpression, and TNBC were 25 (8.10%), 62 (20.06%), 21 (6.80%), and 13 (4.21%), respectively (*Table 1*).

Table 2 compares differences in the six indicators, including longitudinal diameter increment, transverse diameter increment, area increment, percent increase in longitudinal diameter, percent increase in transverse diameter, and percent increase in area increment, between benign and malignant lesions. After enhancement, all six indicators were significantly higher in malignant than in benign lesions (all P<0.05). The results of logistic regression in exploring independent risk factors for diagnosis of malignant masses by CEUS are shown in *Table 3*. The area increment was the optimal indicator among the six parameters [odds ratio (OR): 35.30; P<0.001]. A ROC curve was plotted by comparing the area increment with pathological findings, and the cutoff value was determined based on the Jorden index to distinguish between benign and malignant nodules (*Figure 2*). The area under the curve (AUC), sensitivity, specificity, accuracy, positive predictive value, and negative predictive value for distinguishing between benign and malignant breast nodules by CEUS were 0.945, 90.1% (109/121), 91.5% (172/188), 90.9%

Table 2 Differences in expanded range after enhancement of lesions compared between benign and malignant lesions

Factors	Benign lesion (n=188)	Malignant lesion (n=121)	P value
Longitudinal diameter increment (mm)	0.70±0.94	2.48±2.24	<0.001
Transverse diameter increment (mm)	0.28±1.33	6.06±4.33	<0.001
Area increment (cm^2)	0.13±0.24	1.53±0.96	<0.001
Percent increase in longitudinal diameter (%)	7.40±10.10	18.96±17.14	<0.001
Percent increase in transverse diameter (%)	1.81±8.54	34.64±27.63	<0.001
Percent increase in area increment (%)	9.85±16.56	76.25±48.22	<0.001

Measurement data (e.g., age) are presented as the mean ± SD. SD, standard deviation.

Table 3 Binary logistic regression analysis to identify malignant lesions

Factors	OR (95% CI)	P value
Longitudinal diameter increment (mm)	1.15 (0.55–2.42)	0.709
Transverse diameter increment (mm)	0.91 (0.51–1.64)	0.761
Area increment (cm^2)	35.30 (6.25–199.23)	<0.001
Percent increase in longitudinal diameter (%)	0.97 (0.90–1.06)	0.547
Percent increase in transverse diameter (%)	1.06 (0.96–1.17)	0.228
Percent increase in area increment (%)	1.02 (0.99–1.05)	0.176

OR, odds ratio; CI, confidence interval.

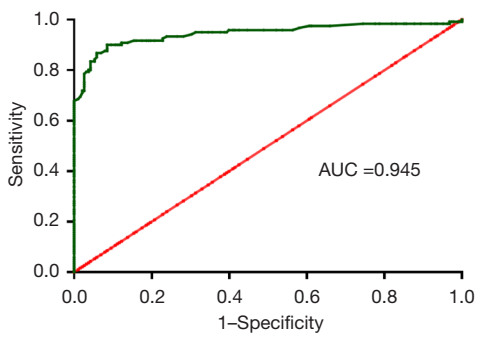

Figure 2 ROC curve of the area increment after enhancement of lesions. AUC, the area under the curve; ROC, receiver operating characteristic.

(281/309), 87.2% (109/125), and 93.5% (172/184), respectively, when the area increment was greater than the cutoff value (0.47 cm^2). As shown in *Figure 3*, the enhanced area of malignant breast nodules increased significantly after enhancement, whereas the enhanced area of benign nodules did not change notably.

Correlations between the pathological maximum diameter of breast cancer and the six indicators are shown in *Table 4*. The correlation coefficients for the area increment, percent increase in transverse diameter, and percent increase in area increment were 0.38, −0.19 and −0.25, respectively, which were statistically significant (all P<0.05). *Tables 5*,*6* compare differences in these six indicators among different molecular subtypes and between two pathological grade groups of breast cancer, respectively. Different molecular subtypes significantly differed in the longitudinal diameter increment and percent increase in longitudinal diameter. Further pairwise comparisons showed that the longitudinal diameter increment in the luminal A group was significantly smaller than that in the HER2+ group, though the percent increase in longitudinal diameter showed no significant difference; in contrast, the percent increase in transverse diameter in the grade I–II group was significantly larger than that in the grade III group (P<0.05) (*Figure 4*). As depicted in *Figure 5*, a ROC curve was constructed for the percent increase in transverse diameter. The AUC, sensitivity, specificity, accuracy, positive predictive value, and negative predictive value for pathological grading by CEUS were 0.623, 90.8% (59/65), 35.7% (20/56), 65.3%

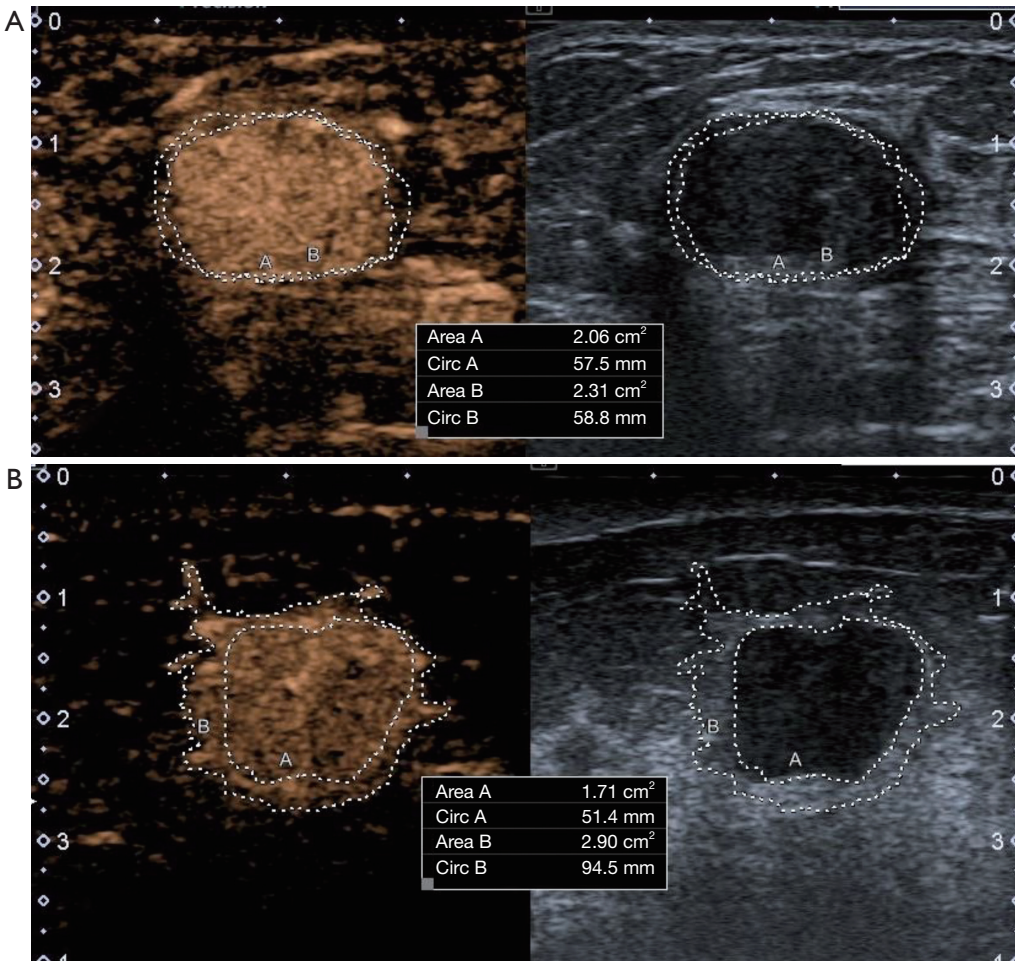

Figure 3 The area of lesion increment after enhancement. (A) In a 33-year-old female with FA, the area increment was not obvious after enhancement (compared with conventional ultrasound). (B) In a 71-year-old female, the area increment of the IDC was 1.19 cm^2 after enhancement. FA, fibroadenoma; IDC, invasive ductal carcinoma.

Table 4 Correlation analysis between pathologic maximum diameter and expanded range after enhancement of malignant lesions

Factors	Pathologic maximum diameter	
	r	P value
Longitudinal diameter increment (mm)	0.12	0.181
Transverse diameter increment (mm)	0.03	0.743
Area increment (cm^2)	0.38	<0.001
Percent increase in longitudinal diameter (%)	−0.07	0.418
Percent increase in transverse diameter (%)	−0.19	0.035
Percent increase in area increment (%)	−0.25	0.007

(79/121), 62.1% (59/95), and 76.9% (20/26), respectively, when the cutoff value was 10.84% based on the Jorden index.

Discussion

In the present study, we analyzed the performance of six indicators of expanded range after enhancement (including longitudinal diameter increment, transverse diameter increment, percent increase in longitudinal diameter, percent increase in transverse diameter, area increment, and percent increase in area increment) in distinguishing benign from malignant masses and in predicting the prognosis of malignant lesions. Malignant lesions had a more obviously expanded range after enhancement than

Table 5 Differences in the expanded range after enhancement of malignant lesions compared among different molecular types

Factors	Luminal A (n=25)	Luminal B (n=62)	HER2+ (n=21)	TNBC (n=13)	P value
Longitudinal diameter increment (mm)	1.37±2.18	2.53±2.19	3.45±2.44	2.85±1.47	0.015
Transverse diameter increment (mm)	5.68±4.43	6.13±4.26	6.14±4.89	6.32±3.99	0.967
Area increment (cm^2)	1.10±0.80	1.61±0.91	1.81±1.18	1.50±0.86	0.059
Percent increase in longitudinal diameter (%)	13.10±19.88	18.50±16.36	23.94±15.36	24.33±15.65	0.039
Percent increase in transverse diameter (%)	40.64±33.91	34.41±26.67	26.01±20.21	38.15±28.65	0.332
Percent increase in area increment (%)	71.79±53.95	80.64±48.06	62.97±40.44	85.30±49.23	0.352

Measurement data (e.g., age) are presented as the mean ± SD. HER2, human epidermal growth factor receptor 2; TNBC, triple-negative breast cancer; SD, standard deviation.

Table 6 Differences in the expanded range after enhancement of malignant lesions compared among different pathological grades

Factors	Grade I–II (n=65)	Grade III (n=56)	P value
Longitudinal diameter increment (mm)	2.18±2.26	2.83±2.19	0.110
Transverse diameter increment (mm)	6.41±4.07	5.66±4.62	0.343
Area increment (cm^2)	1.41±0.89	1.67±1.01	0.127
Percent increase in longitudinal diameter (%)	17.36±17.84	20.80±16.24	0.253
Percent increase in transverse diameter (%)	39.43±27.24	29.09±27.28	0.020
Percent increase in area increment (%)	79.22±46.43	72.79±50.41	0.308

Measurement data (e.g., age) are presented as the mean ± SD. SD, standard deviation.

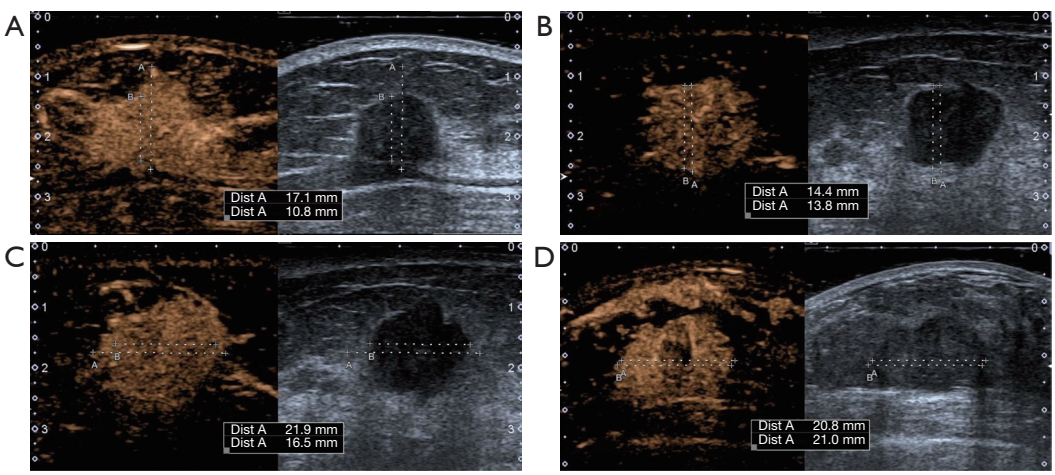

Figure 4 The longitudinal diameter increment and the percentage increase in the transverse diameter of lesion after enhancement. (A) In a 48-year-old female with HER2+ breast cancer, the longitudinal diameter increment of her IDC was 6.3 mm after enhancement. (B) In a 71-year-old female with luminal A breast cancer, the longitudinal diameter increment of IDC was 0.6 mm after enhancement. (C) In a 70-year-old female with grade II breast cancer, the percentage increase in the transverse diameter of IDC was 32.7% after enhancement. (D) In a 36-year-old female with grade III breast cancer, the percent increase in the transverse diameter of IDC was 1.0% after enhancement. HER2, human epidermal growth factor receptor 2; IDC, invasive ductal carcinoma.

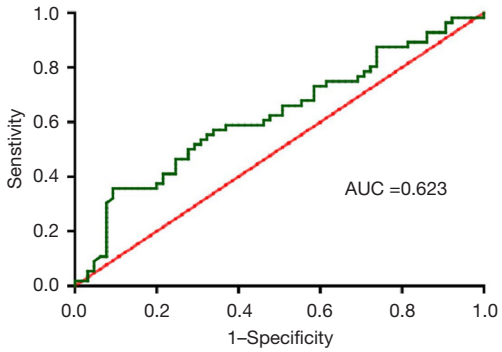

Figure 5 ROC curve of the percentage increase in transverse diameter after enhancement of lesions. AUC, the area under the curve; ROC, receiver operating characteristic.

benign lesions, especially in terms of area increment. The pathologically measured maximum diameter of malignant masses correlated with the percent increase in transverse diameter, area increment, and percent increase in area increment. The longitudinal diameter increment of luminal A breast cancer was smaller than those of other molecular subtypes and significantly smaller than that of HER2-positive breast cancer. Comparison between grades I–II and grade III groups revealed that the percent increase in transverse diameter helped to predict the pathological grade of malignant masses.

The expanded range after enhancement is key evidence for distinguishing a benign from a malignant breast tumor (12,13). The present study further confirmed this and found that the area increment was highly valuable. In fact, the morphologies and distribution of vessels differ between the peripheral and central areas of malignant tumors, but there is no such difference in the vascularity and perfusion between the peripheral and central areas of benign masses. The microvessel density (MVD) and expression of vascular endothelial growth factor (VEGF) and human kinase insert domain-containing receptor (KDR) are significantly higher in the peripheral area of malignant lesions than in the central area (14). Fujimitsu *et al.* (15) believed that under the ultrasonographic enhancement pattern, the Axk value (Axk defined as the slope of the tangent at the beginning of the time-intensity curve) was significantly associated with the final diagnosis of a benign or malignant lesion. Currently, most studies qualitatively describe the increase in the extent of ultrasonographic enhancement to determine the benignity or malignancy of masses, but few quantitative analyses have been performed. In our study, we found that the sensitivity, specificity, and accuracy of area increment were high (90.1%, 91.5%, and 90.9%, respectively) at a cutoff value of 0.47 cm^2, showing notable clinical relevance.

Molecular typing of breast cancer is important for prognostic prediction. Patients with luminal A breast cancer have a better prognosis than those with other subtypes (16). Wen *et al.* (17) found that all four molecular subtypes of breast cancer exhibited an increased area after enhancement, but no further study was performed. In our current study, we demonstrate by CEUS that the longitudinal diameter increment of luminal A breast cancer is smaller than that of other molecular subtypes and significantly smaller than that of HER2+ breast cancer, indicating that luminal A breast cancer has a smaller infiltration area, better biological behavior, and lower malignancy than other subtypes.

We also found that the percent increase in transverse diameter is helpful in predicting the pathological grade of malignant masses. Zhao *et al.* (18) suggested that some CEUS features (e.g., degree of enhancement, order-of-magnitude enhancement, enhancement pattern, enlarged area of enhancement, and penetrating vessels) of breast cancer of different sizes may be associated with prognostic factors, which may help in prognostic assessment. Conti *et al.* (19) proposed that radiomics are highly promising in predicting the pathological grade of breast cancer. Au *et al.* (20) demonstrated a significant correlation between the marginal and posterior features of breast cancer on ultrasonography and pathological grade. Li *et al.* (21) proposed that the enhancement pattern and parameters of CEUS can indirectly guide the pathological grading of breast cancer and help to evaluate the biological behavior and prognosis of these tumors. In our study, the percent increase in transverse diameter was used to quantitatively analyze and predict pathological grade. Grade I or II breast cancer was found to have a greater percent increase in transverse diameter than grade III. Furthermore, a cutoff value of 10.84% yielded a sensitivity of up to 90.8% in pathological grading, along with a specificity and an accuracy of 35.7% and 65.3%, respectively. Thus, the percent increase in transverse diameter can be used in predicting treatment and prognosis for breast cancer patients. Measurements such as longitudinal diameter increment, transverse diameter increment, area increment, percentage longitudinal diameter increment, transverse diameter increment, and area increment mentioned in this study can distinguish benign and malignant masses without the use of sophisticated quantitative techniques and artificial intelligence models, enabling enhanced contrast-enhanced

ultrasound to be used in daily clinical diagnosis.

Recently, Artificial intelligence (AI) -powered ultrasound has been applied increasingly in clinical breast lesion evaluation, which can assist to improve image acquisition, evaluate image quality and diagnose lesions (22). But at present, AI's main interest in breast ultrasound is to detect and distinguish benign and malignant breast masses by morphological and textural features based on the features of gray scale ultrasound (23). There are no researchers who have built machine-learning models for CEUS characteristics. This study found that the indicators related to the expansion of lesion scope in contrast-enhanced ultrasound are helpful for the differential diagnosis of benign and malignant lesions as well as the prognosis assessment of pathological grades. If combined with machine learning, it is believed that it will have a broader clinical application prospect.

Of course, our current study also had some limitations. (I) This study was a single-center retrospective study, and its findings need validation and promotion in multi-institutional studies. (II) The sample size for evaluating tumor volume was relatively small and needs to be expanded to increase reliability. (III) Some other lesions, such as ductal carcinoma in situ (DCIS) and nonmass-like lesions (NMLs), which have blurred boundaries, were not included in this study and need to be explored in follow-up studies. (IV) Multiple indicators on CEUS are meaningful for differentiation of benign and malignant masses and for assessing prognosis of patients with malignant lesions. Overall, combined assessment using these indicators can help to improve diagnostic performance.

Conclusions

In this single-center retrospective study, we conducted an in-depth analysis of indicators of expanded lesion range on CEUS and found that these indicators are helpful in differential diagnosis of benign and malignant lesions and in prognostic assessment of pathological grade.

Acknowledgments

Funding: None.

Footnote

Reporting Checklist: The authors have completed the STARD reporting checklist. Available at https://gs.amegroups.com/article/view/10.21037/gs-23-165/rc

Data Sharing Statement: Available at https://gs.amegroups.com/article/view/10.21037/gs-23-165/dss

Peer Review File: Available at https://gs.amegroups.com/article/view/10.21037/gs-23-165/prf

Conflicts of Interest: All authors have completed the ICMJE uniform disclosure form (available at https://gs.amegroups.com/article/view/10.21037/gs-23-165/coif). The authors have no conflicts of interest to declare.

Ethical Statement: The authors are accountable for all aspects of the work in ensuring that questions related to the accuracy or integrity of any part of the work are appropriately investigated and resolved. The study was conducted in accordance with the Declaration of Helsinki (as revised in 2013). The study was approved by institutional ethics board of Shanghai General Hospital (No. 2016KY221) and individual consent for this retrospective analysis was waived.

References

1. Sung H, Ferlay J, Siegel RL, et al. Global Cancer Statistics 2020: GLOBOCAN Estimates of Incidence and Mortality Worldwide for 36 Cancers in 185 Countries. CA Cancer J Clin 2021;71:209-49.
2. Bray F, Jemal A, Grey N, et al. Global cancer transitions according to the Human Development Index (2008-2030): a population-based study. Lancet Oncol 2012;13:790-801.
3. Berg WA, Bandos AI, Mendelson EB, et al. Ultrasound as the Primary Screening Test for Breast Cancer: Analysis From ACRIN 6666. J Natl Cancer Inst 2016;108:djv367.
4. Tagliafico AS, Mariscotti G, Valdora F, et al. A prospective comparative trial of adjunct screening with tomosynthesis or ultrasound in women with

mammography-negative dense breasts (ASTOUND-2). Eur J Cancer 2018;104:39-46.
5. Li YJ, Wen G, Wang Y, et al. Perfusion heterogeneity in breast tumors for assessment of angiogenesis. J Ultrasound Med 2013;32:1145-55.
6. Kuczynski EA, Vermeulen PB, Pezzella F, et al. Vessel co-option in cancer. Nat Rev Clin Oncol 2019;16:469-93.
7. Li Q, Hu M, Chen Z, et al. Meta-Analysis: Contrast-Enhanced Ultrasound Versus Conventional Ultrasound for Differentiation of Benign and Malignant Breast Lesions. Ultrasound Med Biol 2018;44:919-29.
8. Wang Y, Fan W, Zhao S, et al. Qualitative, quantitative and combination score systems in differential diagnosis of breast lesions by contrast-enhanced ultrasound. Eur J Radiol 2016;85:48-54.
9. Shima H, Okuno T, Nakamura T, et al. Comparing the extent of breast cancer tumors through contrast-enhanced ultrasound vs B-mode, opposed with pathology: evergreen study. Breast Cancer 2021;28:405-13.
10. Sanati S. Morphologic and Molecular Features of Breast Ductal Carcinoma in Situ. Am J Pathol 2019;189:946-55.
11. Amin M, Edge S, Greene F, et al. AJCC (American Joint Committee on Cancer) Cancer Staging Manual. 8th ed. Chicago, IL: Springer; 2018.
12. Liu G, Zhang MK, He Y, et al. BI-RADS 4 breast lesions: could multi-mode ultrasound be helpful for their diagnosis? Gland Surg 2019;8:258-70.
13. Xiao X, Ou B, Yang H, et al. Breast contrast-enhanced ultrasound: is a scoring system feasible? A preliminary study in China. PLoS One 2014;9:e105517.
14. Park AY, Kwon M, Woo OH, et al. A Prospective Study on the Value of Ultrasound Microflow Assessment to Distinguish Malignant from Benign Solid Breast Masses: Association between Ultrasound Parameters and Histologic Microvessel Densities. Korean J Radiol 2019;20:759-72.
15. Fujimitsu R, Shimakura M, Urakawa H, et al. Homogeneously enhancing breast lesions on contrast enhanced US: differential diagnosis by conventional and contrast enhanced US findings. Jpn J Radiol 2016;34:508-14.
16. Gao JJ, Swain SM. Luminal A Breast Cancer and Molecular Assays: A Review. Oncologist 2018;23:556-65.
17. Wen B, Kong W, Zhang Y, et al. Association Between Contrast-Enhanced Ultrasound Characteristics and Molecular Subtypes of Breast Cancer. J Ultrasound Med 2022;41:2019-31.
18. Zhao LX, Liu H, Wei Q, et al. Contrast-Enhanced Ultrasonography Features of Breast Malignancies with Different Sizes: Correlation with Prognostic Factors. Biomed Res Int 2015;2015:613831.
19. Conti A, Duggento A, Indovina I, et al. Radiomicsin breast cancer classification and prediction. Semin Cancer Biol 2021;72:238-50.
20. Au FW, Ghai S, Lu FI, et al. Histological Grade and Immunohistochemical Biomarkers of Breast Cancer: Correlation to Ultrasound Features. J Ultrasound Med 2017;36:1883-94.
21. Li X, Li Y, Zhu Y, et al. Association between enhancement patterns and parameters of contrast-enhanced ultrasound and microvessel distribution in breast cancer. Oncol Lett 2018;15:5643-9.
22. Akkus Z, Cai J, Boonrod A, et al. A Survey of Deep-Learning Applications in Ultrasound: Artificial Intelligence-Powered Ultrasound for Improving Clinical Workflow. J Am Coll Radiol 2019;16:1318-28.
23. Bitencourt A, Daimiel Naranjo I, Lo Gullo R, et al. AI-enhanced breast imaging: Where are we and where are we heading? Eur J Radiol 2021;142:109882.

Cite this article as: Jia C, Niu Q, Liu L, Li G, Jin L, Du L, Shi Q, Li F. Value of an expanded range of lesions on contrast-enhanced ultrasound for the diagnosis of hypervascular breast masses. Gland Surg 2023;12(6):824-833. doi: 10.21037/gs-23-165